
Article:
Ferraiuoli, P., Fixsen, L.S., Kappler, B. et al. (3 more authors) (2019) Measurement of in vitro cardiac deformation by means of 3D digital image correlation and ultrasound 2D speckle-tracking echocardiography. Medical Engineering & Physics. ISSN 1350-4533

https://doi.org/10.1016/j.medengphy.2019.09.021

Medical Engineering and Physics xxx (xxxx) xxx

Contents lists available at ScienceDirect

Medical Engineering and Physics

journal homepage: www.elsevier.com/locate/medengphy

Measurement of *in vitro* cardiac deformation by means of 3D digital image correlation and ultrasound 2D speckle-tracking echocardiography

Paolo Ferraiuoli[a,b,1], Louis S. Fixsen[c,1], Benjamin Kappler[d,e,1], Richard G.P. Lopata[c], John W. Fenner[a,b], Andrew J. Narracott[a,b,*]

[a] *Mathematical Modelling in Medicine Group, Department of Infection, Immunity and Cardiovascular Disease, University of Sheffield, Sheffield, United Kingdom*
[b] *Insigneo Institute for in silico medicine, University of Sheffield, Sheffield, United Kingdom*
[c] *Cardiovascular Biomechanics group, Department of Biomedical Engineering, Eindhoven University of Technology, Eindhoven, Netherlands*
[d] *LifeTec Group B.V., Eindhoven, Netherlands*
[e] *Amsterdam University Medical Center, Department Cardiothoracic Surgery, Amsterdam, Netherlands*

ARTICLE INFO

Article history:
Received 31 January 2019
Revised 26 July 2019
Accepted 29 September 2019
Available online xxx

Keywords:
Biomechanics
3D digital image correlation
Ultrasound 2D speckle-tracking echocardiography
Cardiac displacement and strain
in vitro porcine heart

ABSTRACT

Ultrasound-based 2D speckle-tracking echocardiography (US-2D-STE) is increasingly used to assess the functionality of the heart. In particular, the analysis of cardiac strain plays an important role in the identification of several cardiovascular diseases. However, this imaging technique presents some limitations associated with its operating principle that result in low accuracy and reproducibility of the measurement.

In this study, an experimental framework for multimodal strain imaging in an *in vitro* porcine heart was developed. Specifically, the aim of this work was to analyse displacement and strain in the heart by means of 3D digital image correlation (3D-DIC) and US-2D-STE. Over a single cardiac cycle, displacement values obtained from the two techniques were in strong correlation, although systematically larger displacements were observed with 3D-DIC. Notwithstanding an absolute comparison of the strain measurements was not possible to achieve between the two methods, maximum principal strain directions computed with 3D-DIC were consistent with the longitudinal and circumferential strain distribution measured with US-2D-STE. 3D-DIC confirmed its high repeatability in quantifying displacement and strain over multiple cardiac cycles, unlike US-2D-STE which is affected by accumulated errors over time (i.e. drift).

To conclude, this study demonstrates the potential of 3D-DIC to perform dynamic measurement of displacement and strain during heart deformations and supports future applications of this method in *ex vivo* beating heart platforms, which replicate more fully the complex contraction of the heart.

1. Introduction

Cardiovascular diseases (CVDs) remain the leading cause of death worldwide accounting for 31% of all global deaths in 2015 [1]. The evaluation of left ventricular (LV) systolic strain plays an important role in establishing prognosis and treatment strategies for several CVDs [2]. LV global longitudinal strain (GLS) has proved to be a robust and reproducible marker to detect cardiac pathologies that other clinical parameters such as the LV ejection fraction (LVEF) may not reveal [2]. Namely, the assessment of LV GLS may predict significant coronary heart disease, assess systolic function in ventricles with hypertrophy, indicate risk of diabetic cardiomyopathy and support early detection of sub-clinical LV dysfunction. Different non-invasive imaging techniques can be used to perform cardiac strain imaging (CSI) [3] such as ultrasound speckle-tracking echocardiography (STE), cardiac magnetic resonance imaging (cMRI) and cardiac computed tomography (CCT). Despite the status of cMRI as the gold standard for the quantification of myocardial strain, its application is limited mainly to academic research due to several restrictions (e.g., hardware

* Corresponding author at: Mathematical Modelling in Medicine Group, Department of Infection, Immunity & Cardiovascular Disease, Faculty of Medicine, Dentistry & Health, University of Sheffield, Medical School, Beech Hill Road, Sheffield, S10 2RX, UK.
E-mail addresses: p.ferraiuoli@sheffield.ac.uk (P. Ferraiuoli), a.j.narracott@sheffield.ac.uk (A.J. Narracott).
[1] These authors contributed equally to this publication.

https://doi.org/10.1016/j.medengphy.2019.09.021

cost, long and complex scanning protocols, claustrophobia and contraindications for patients with certain implanted devices).

The most widely used technique for CSI assessment is ultrasound 2D-STE (US-2D-STE) [3], which processes US planar cross-sectional views of the heart obtained from constructive and destructive interferences of US waves with the tissue structure. Use of multiple views reduces dependence on insonation angle and allows measurements of different myocardial strain components (e.g., longitudinal, circumferential and radial) irrespective of the direction of the beam. However, although US-2D-STE is a very useful technique and its accuracy has been validated *in vitro* against sonomicrometry and *in vivo* against cMRI, accurate tissue tracking largely depends on the US image quality, which typically has a low signal to noise ratio [4]. Furthermore, image quality is known to vary along the US beam, with improved tracking quality close to the US probe, thereby limiting accuracy and reproducibility, although this can be mitigated by averaging strain. This implies that local results are less accurate than global measures. In addition, the inherent limitations of 2D imaging are present in US-2D-STE, for instance, the use of foreshortened views and geometric assumptions that tissues displace only within the 2D imaging plane, while the heart undergoes complex 3D motion. Whilst US-3D-STE is emerging as a promising technique to circumvent these issues, it is still under development and verification and has a considerably lower spatial and temporal resolution than US-2D-STE [4].

3D digital image correlation (3D-DIC), an optical-numerical method [5], has become an important tool to characterise the mechanical behaviour of cardiovascular tissues [6]. For example, Sutton et al. [7] measured surface strain fields on mouse carotid arteries combining a stereomicroscope and 3D-DIC. Genovese et al. [8] developed an optical system including DIC to describe the asymmetrical deformations exhibited by a porcine ventricular myocardium in response to an indentation test. Bersi et al. [9] collected full-field biaxial data using a panoramic DIC system to perform an inverse characterisation of regional variation in the properties of murine aortas. Moreover, 3D-DIC has been applied in the CSI field to assess the behaviour of the right ventricle in humans [10]. In that work, *in vivo* measurement was achieved, as the heart surface was visible during open-chest bypass surgery. However, the complexity of the study did not allow an adequate investigation of 3D-DIC accuracy and reproducibility for cardiac strain measurements. Thus, recently, we explored the feasibility of applying 3D-DIC in an *in vitro* heart model, which ensured reproducible and physiological haemodynamic conditions [11]. Results obtained showed highly accurate and repeatable measurements of high-resolution strain on the epicardial surface. Furthermore, this previous study demonstrated the potential for multimodal strain imaging of the heart.

The aim of the current study was to assess and compare the performance of 3D-DIC and US-2D-STE to analyse displacement and strain in the *in vitro* heart model described previously [11,12] and, ultimately, to provide further reference measurements that may support the ongoing validation process of clinical imaging modalities for cardiac strain evaluation.

2. Materials and methods

2.1. Platform preparation

The Cardiac BioSimulator (CBS, LifeTec Group B.V., Eindhoven, NL) platform was prepared following the same procedure described previously [11,12] and four porcine hearts were considered in the *in vitro* testing. Different dynamic loading conditions were applied to the heart to reproduce a normotensive (NT) haemodynamic condition (mean atrial pressure and mean aortic pressure of 15 mmHg and 100 mmHg, respectively) and a hypertensive condition (HT) (mean atrial pressure and mean aortic pressure of 15 mmHg and 130 mmHg, respectively) [13]. To compare 3D-DIC and US-2D-STE, the experimental protocol was designed to accommodate the requirements of the two techniques and improve their image quality. Specifically, the heart was placed on a soft support within a tank, which was filled in a saline solution to submerge the heart when US-2D-STE was performed. Whereas, when 3D-DIC was carried out, the tank was drained and the heart was left in air. Fig. 1 shows a schematic representation of the experimental setup.

2.2. 3D-DIC analysis

Before placing the heart in the platform, an artificial speckle pattern was created on the LV surface as previously described [11,14]. Specifically, a methylene blue solution (Sigma-Aldrich Company Ltd, Dorset, UK) was applied on the epicardium to create a dark background, enhancing contrast with random white speckles applied using an airbrush (Iwata Hi-Line HP-CH, Anest Iwata-Medea Inc., Portland, OR, US) and water-based acrylic paint (Com-Art, Anest Iwata-Medea Inc., Portland, OR, US). Speckle pattern quality was assessed through a morphological analysis [15] using custom Matlab (Matlab R2015b, Mathworks, Natick, MA, US) codes.

Two 8-bit digital CCD cameras (Flea2–13S2, Point Grey Research Inc., Vancouver, Canada) were arranged in a stereo configuration

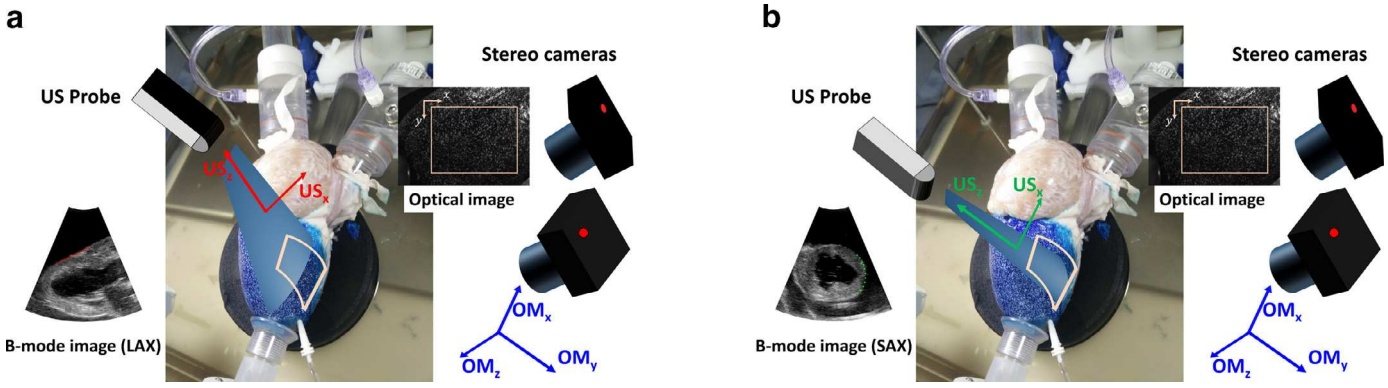

Fig. 1. Schematic representation of the experimental setup. The figure shows roughly the position and orientation of the US probe coordinate system, for the LAX (a) and SAX views (b), along with the stereo cameras coordinate system respect to the heart. Illustration of the corresponding B-mode and optical images acquired by the two methods are illustrated on the left and right sides, respectively. US beam and the ROI selected for the 3D-DIC analysis are overlaid on the heart surface to show the approximate region of overlap between the two techniques.

Please cite this article as: P. Ferraiuoli, L.S. Fixsen and B. Kappler et al., Measurement of in vitro cardiac deformation by means of 3D digital image correlation and ultrasound 2D speckle-tracking echocardiography, Medical Engineering and Physics, https://doi.org/10.1016/j.medengphy.2019.09.021

Table 1
Camera parameters and DIC settings.

Camera parameters	Value
Camera resolution [pixels]	1024×768
Image resolution [mm/pixels]	0.1
Magnification	0.05
DIC settings	
Software	Ncorr
Subset size [pixels]	33
Step size [pixels]	9
Interpolation	Biquintic B-spline
Shape function	First-order

(baseline distance of 200 mm and stereo angle of approximately 15°) to capture synchronised images pairs at 30 frames per second (fps) of the heart during its deformation. To avoid motion blur of the speckles, a reduced shutter speed (5 ms) was set, whilst requiring the use of additional lighting. In fact, a white-light LED lamp was used to improve lighting conditions and avoid flickering. The cameras were placed roughly 1 m away from the platform and with magnifications adjusted to ensure the whole region of the lateral LV surface was imaged. Upon completion of the experiment, the cameras were calibrated by capturing 20 images of a flat chequerboard made of 2 mm internal squares and using the Matlab Stereo Camera Calibrator Application. Camera parameters and DIC settings are reported in Table 1.

The workflow designed for 3D-DIC analysis has been previously reported [11]. Briefly, after selecting a region of interest (ROI) in the optical image of the lateral LV surface as shown in Fig. 1, the 3D-DIC analysis was carried out using the Ncorr program [16] and custom Matlab codes. From the reconstruction of 3D points on the LV surface, displacement and strain were computed with respect to a reference state corresponding to the maximum loading condition in the LV. Strain fields on the reconstructed surfaces were obtained by computing the deformations of triangular elements defined on the surface mesh between the reference and deformed states. Deformations within the triangular elements were assumed to be homogeneous [17,18]. From the deformation gradient tensor (**F**), the Green-Lagrange strain tensor (**E**) was calculated using the equation $\mathbf{E} = (\mathbf{F}^t\mathbf{F} - \mathbf{I})/2$. Finally, by solving the eigenvalue/eigenvector problem of the local strain tensor, the magnitude and direction of the maximum and minimum principal strains were obtained.

2.3. US-2D-STE analysis

US-2D-STE data were acquired using a MyLab70 XVG US system (Esaote, Maastricht, NL) and a curved array transducer (centre frequency of 2.7 MHz and 55-degree opening angle). An imaging depth of 130 mm was used, resulting in a frame rate of 47 Hz. Radio-frequency (RF) data were acquired at the mid-level of the heart, halfway between the apex and mitral valve, with the papillary muscles visible. Images of the LV were acquired in the cross-sectional short-axis (SAX) and the longitudinal-axis (LAX) view by rotating the probe 90°.

Data were imported into Matlab for displacement tracking and strain estimation. The sequences of RF data were first segmented into clips of at least four heart cycles, based on M-mode of the LV centre-line. Displacement tracking was performed using the 'coarse-to-fine' algorithm, previously published by Lopata et al. [19]. The method uses a window of RF data that reduces in size over three iterations. Displacements were estimated in both the axial (in the US beam path) and lateral (across the lines of RF data) directions. Prior to displacement estimation, the endocardial and epicardial borders of the LV were segmented, and a mesh of 11 radial and 91 circumferential coordinates generated covering the segmented region. The mesh was annular in shape for the SAX view and U-shaped in the LAX view. The points of the mesh were tracked based on the obtained displacement field. The cavity surface area was calculated from the inner contour of the mesh. Start- and end-points of the sequence were shortened to peaks in the surface area. Strain was calculated by taking the spatial derivative of the deformation of the mesh from the initially segmented geometry using a least-squares strain estimator [20], in the true local directions. Circumferential strain was calculated in the SAX view, longitudinal strain in the LAX view. Radial strain was calculated in both views.

2.4. Data analysis and comparison between the two techniques

Before comparing results from the two imaging modalities, a performance assessment of 3D-DIC was undertaken to evaluate its accuracy and repeatability. To preserve camera calibration accuracy and due to constraints imposed by the pump, the established test to assess strain error [21] was not feasible. However, a metric of deviation from anticipated zero strain was estimated by measuring the strain between multiple images of the heart captured in the un-loaded configuration.

Comparison of cardiac displacement and strain measurements obtained from 3D-DIC and US-2D-STE was conducted for the NT condition over a single cardiac cycle. Specifically, after identifying the points in the US images, in both the LAX and SAX views (Fig. 1a and b, respectively), lying within the optical reconstructed ROI, the US-2D-STE displacement components were extracted and their average and standard deviation were calculated. The same approach was applied to the displacement values retrieved from the 3D-DIC method. Some assumptions are required relating to the relative configuration of US probe and stereo cameras, as shown in Fig. 1 (see supplementary materials for a further illustration of the relative position and orientation of the US imaging plane respect to the stereo camera coordinate system). Comparison between the two methods was undertaken by analysing the displacement along the axial direction of the US beam (z-axis), both in the LAX and SAX views, and the displacement along the y-axis of the left camera. Furthermore, the median values of the displacement from all four hearts over the first cardiac cycle was calculated and the correlation between 3D-DIC and US-2D-STE, for the two views, was evaluated. Concerning the strain measurements, average and standard deviation were computed for both the maximum and minimum principal strains over the ROI reconstructed with 3D-DIC and the longitudinal and circumferential strains derived from US-2D-STE in the LAX and SAX views, respectively.

3. Results

From the morphological analysis of the speckle pattern was observed that most of the speckles (roughly 70%) had a size of 4 ± 1 pixels, which belonged to the recommended range to avoid aliasing (3–5 pixels [5]). Mean reprojection errors, a qualitative measure of cameras calibration accuracy, were typically 0.16 pixels (0.016 mm) across the experiments.

Fig. 2 illustrates a dynamic representation of the 3D displacement components of the four hearts obtained from 3D-DIC at the NT (solid lines) and HT (dashed lines) conditions. Specifically, this plot shows the average of each displacement component (X, Y and Z) within the ROI on the epicardial surface along four cardiac cycles. Fig. 3a depicts the B-mode images of LAX and SAX views for each individual heart indicating the region (dotted lines) used to extract displacement and strain, estimated to correspond to the ROI imaged by the stereo cameras. Displacement curves showing average and standard deviation over a single cardiac cycle computed with 3D-DIC and US-2D-STE, for every heart, are reported

Please cite this article as: P. Ferraiuoli, L.S. Fixsen and B. Kappler et al., Measurement of in vitro cardiac deformation by means of 3D digital image correlation and ultrasound 2D speckle-tracking echocardiography, Medical Engineering and Physics, https://doi.org/10.1016/j.medengphy.2019.09.021

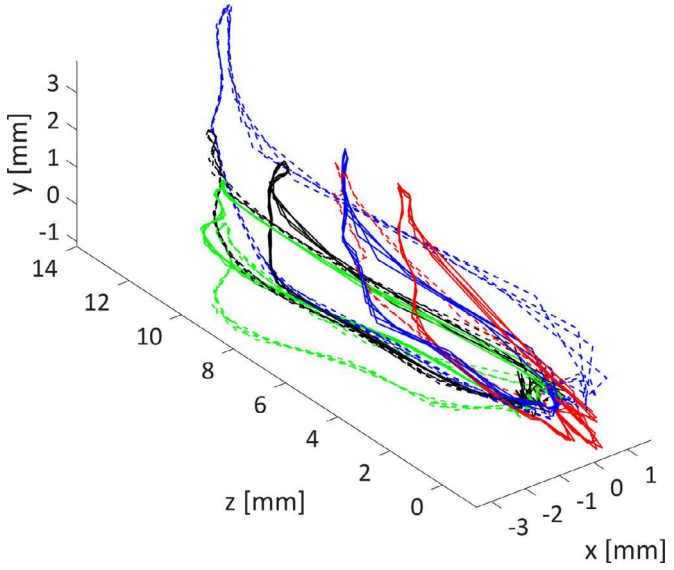

Fig. 2. Representation of the dynamic displacement of the four hearts (each heart is associated with a different colour) in 3D along four cardiac cycles measured by 3D-DIC. The solid and dashed lines were obtained as the average of the displacement components (x, y and z) at each state of the heart deformations for the NT and HT condition, respectively.

in Fig. 3b. Median values of peak displacement amongst the four hearts were -7.1 ± 1.9 mm, -5.8 ± 0.1 mm and -5.4 ± 0.1 mm, from 3D-DIC, US-2D-STE LAX and SAX view, respectively. Fig. 3c shows the maximum (E_1) and minimum (E_2) principal strains quantified with 3D-DIC and the longitudinal and circumferential strains obtained from US-2D-STE. Median values at peak strain over all four hearts were $-11.9 \pm 3.3\%$, $0.9 \pm 2.2\%$, $-6.6 \pm 4.4\%$ and $-4.3 \pm 1.4\%$, for E_1, E_2, longitudinal and circumferential strains, respectively. In each individual heart, full-field strains over the ROI reconstructed on the LV surface (Fig. 3d) with 3D-DIC are shown in Fig. 3e. In particular, this figure reports the spatial distribution of E_1 and E_2 over the ROI together with the principal directions at peak strain. As depicted in Fig. 3d, size and position of the reconstructed ROIs were different over the hearts because of changes in the anatomical structures and positioning of the heart respect to the stereo cameras. Overall, width and height of the ROIs ranged between 45 and 60 mm and 35 to 40 mm, respectively. As reported in Fig. 4, displacement data from 3D-DIC showed a very strong correlation with US-2D-STE measurements in both the LAX view ($R^2 = 0.97$) and SAX view ($R^2 = 0.96$). Errors associated with data in Fig. 4 for each technique have not been reported here, however, error metrics from 3D-DIC and US-2D-STE are discussed in the Discussion section.

Results obtained under the HT condition demonstrated similar overall behaviour to those presented in Fig. 3 for the NT condition (see supplementary material for plots). Peak strain values reported for the HT condition were greater than those for the NT condition for most outputs, as shown in Table 2.

4. Discussion

In this study, we have described an experimental framework that enabled direct comparison of ultrasound- and optical-based strain imaging in an *in vitro* heart model. Specifically, the aim of this work was to analyse displacement and strain obtained from 3D-DIC and US-2D-STE in order to evaluate the performance of these techniques.

Estimation of displacement and strain errors, obtained from the 3D-DIC analysis of multiple images of the heart in the unloaded configuration, showed deviations smaller than 6 µm and 1%, respectively, which have been also reported in previous studies [11,14].

Results shown in Fig. 2 demonstrate the ability of 3D-DIC to report the dynamic 3D displacement components of the epicardial surface and further confirm the repeatability of the process over multiple cardiac cycles. This is supported by our previous reports of repeatability in the CBS platform [11] and is in contrast to the typical behaviour observed when tracking displacements over multiple cycles with US-2D-STE resulting in residual tracking errors (i.e. drift) [22].

It should be noted that for the comparison between the two techniques, displacement and strain behaviour were very similar, thus, results were reported in details only for the NT condition. Analysis of displacement values obtained from 3D-DIC and US-2D-STE reported in Fig. 3b shows very good agreement between the two US views and very strong correlation between two techniques, although with consistently larger displacements reported by 3D-DIC, as illustrated in Fig. 4.

Although surface strain fields computed with 3D-DIC were reported in the principal strain configuration to remove coordinate system dependence, an absolute comparison of the strain measurements between these two methods remains challenging to accomplish because of the different nature of the two techniques and procedures used to calculate strain. However, Fig. 3 illustrates that maximum principal strain exceeded both the longitudinal and circumferential strains and minimum principal strain reported was less than either US-2D-STE measurement. This is coherent with the computed direction of the maximum principal strains shown in Fig. 3e, which lies between the longitudinal and circumferential directions consistently for all experiments. This suggests that a component of the increased magnitude of strain reported using 3D-DIC is associated with the orientation of the principal strain direction. It is feasible to repeat such an experiment with a greater number of US views to report strain at multiple angular increments, which would address this issue. However, it is also possible that the 3D motion of the cardiac surface demonstrated in Fig. 2 leads to underestimation of strain in both the LAX and SAX views when using US-2D-STE as it is unable to detect out-of-plane motion.

Despite the two methods share some similarity (i.e. use of template matching algorithms), they do present many differences, especially, on how they calculate and process the displacement in order to derive strain, which makes a direct comparison of spatial resolution challenging. In particular, although US-2D-STE was

Table 2
Peak strain values along a cardiac cycle in each heart measured by 3D-DIC (Maximum and Minimum principal strain) and US-2D-STE (Longitudinal and Circumferential strain) for the NT and HT conditions.

Peak strain [%]	Heart I		Heart II		Heart III		Heart IV	
	NT	HT	NT	HT	NT	HT	NT	HT
Maximum principal strain	−9.0	−11.3	−12.9	−15.2	−14.2	−15.5	−10.9	−13.0
Minimum principal strain	1.5	0.7	0.6	0.9	2.4	1.7	1.5	0.9
Longitudinal strain	−5.4	−8.7	−8.7	−10.6	−7.9	−6.0	−5.4	−7.9
Circumferential strain	−7.1	−6.9	−5.1	−7.0	−3.8	−6.0	−3.2	−7.6

Please cite this article as: P. Ferraiuoli, L.S. Fixsen and B. Kappler et al., Measurement of in vitro cardiac deformation by means of 3D digital image correlation and ultrasound 2D speckle-tracking echocardiography, Medical Engineering and Physics, https://doi.org/10.1016/j.medengphy.2019.09.021

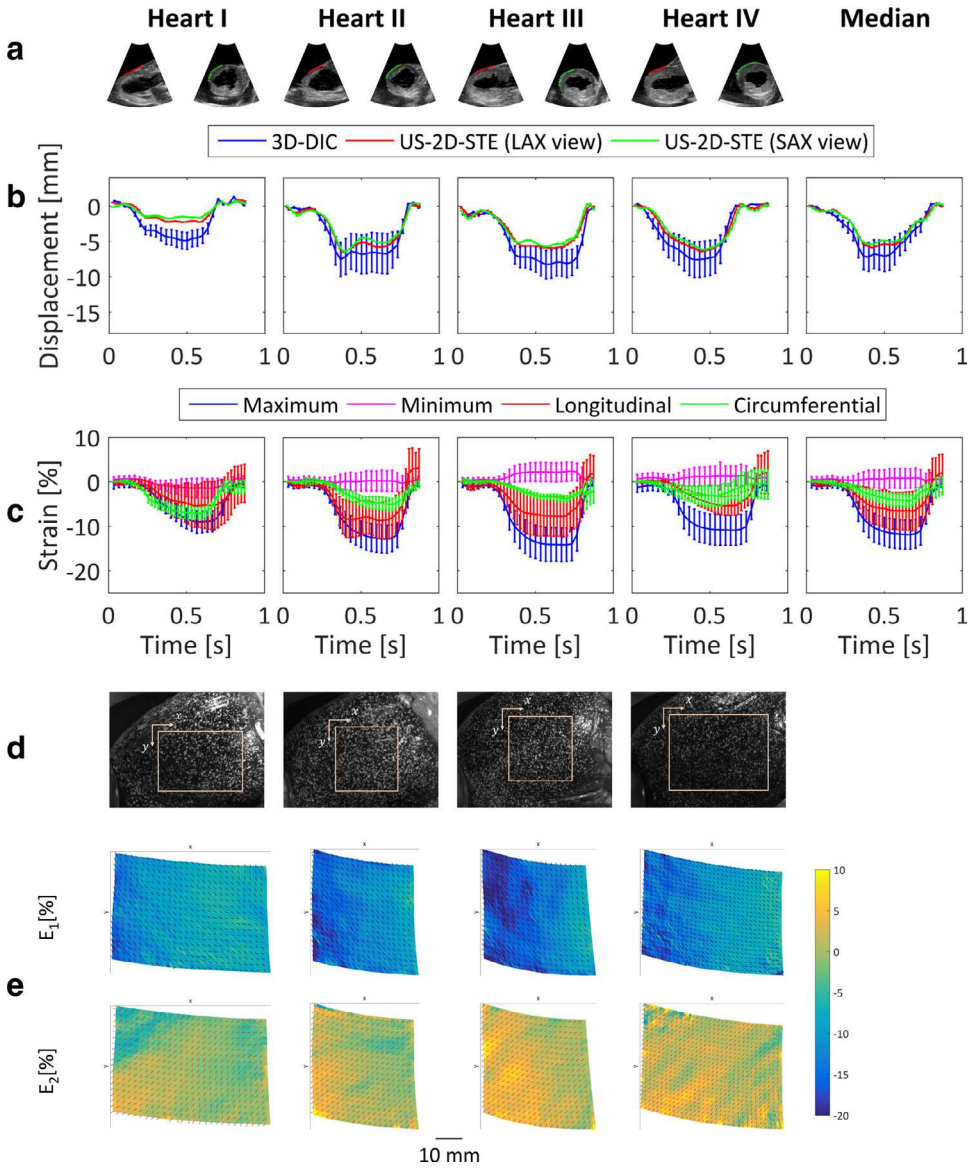

Fig. 3. (a) B-mode image of the LAX and SAX views of each heart with overlaid the points from which displacement and strain were extracted for comparison with 3D-DIC measurements. (b) Average and standard deviation of the displacement distribution extracted from 3D-DIC, US-2D-STE LAX and SAX views in each heart and their median values over a single cardiac cycle. (c) Average and standard deviation for the maximum and minimum principal strains derived from 3D-DIC and the longitudinal and circumferential strains derived from US-2D-STE in each heart and their median values over a single cardiac cycle. (d) Optical images of the LV surface of each individual heart with overlaid a schematic representation of the ROI selected in the 3D-DIC analysis. (e) Magnitude and direction of E_1 and E_2 at peak strain reconstructed with 3D-DIC over the ROI identified in (d).

performed on RF data to improve displacement tracking resolution [19], this is known to vary between the axial and lateral direction. In this study, speckle-tracking resolution, defined by the window size of the last coarse-to-fine iteration, was 3.9 and 20.5 mm in the axial and lateral direction, respectively. However, due to the non-linearity of median filtering to regularise the estimated displacement and the subsequent use of a least-squares strain estimator, an exact quantification of the resulting strain resolution with US-2D-STE was not possible to achieve. Conversely, the evaluation of the spatial resolution of the 3D-DIC measurements reflected the choice of the parameters selected in the DIC analysis. Namely, the subset size accounted for the displacement spatial resolution, which in physical unit resulted $\sim$ 3.3 mm, while strain measurements were reported at a resolution determined by the step size ($\sim$ 0.9 mm).

Moreover, the absence of muscle contractility may explain the lower magnitude of longitudinal and circumferential strain estimated in this study when compared to US-2D-STE strains measurements achieved in isolated beating hearts [22]. Underestimation of US-2D-STE strain, previously observed in another study comparing US-2D-STE with 2D-DIC [23], is a known limitation of US-2D-STE which can be caused by its sensitivity to acoustic shadowing or reverberations, poor image quality and lower accuracy of tissue tracking at the depth associated with cardiac imaging and in the lateral direction [4].

Moreover, the experimental set-up is limited as it was not possible to either acquire 3D-DIC and US-2D-STE image simultaneously or ensure precise alignment of the coordinate systems of the stereo cameras and US probe. Furthermore, it was also necessary to estimate the positions of the reconstructed ROI with 3D-DIC, as shown in Fig. 3d, within the LAX and SAX views, as shown in Fig. 3a, which may introduce some additional uncertainty in direct comparison between the methods. As a result, it is not possible to separate effects associated with inherent measurement errors from

Please cite this article as: P. Ferraiuoli, L.S. Fixsen and B. Kappler et al., Measurement of in vitro cardiac deformation by means of 3D digital image correlation and ultrasound 2D speckle-tracking echocardiography, Medical Engineering and Physics, https://doi.org/10.1016/j.medengphy.2019.09.021

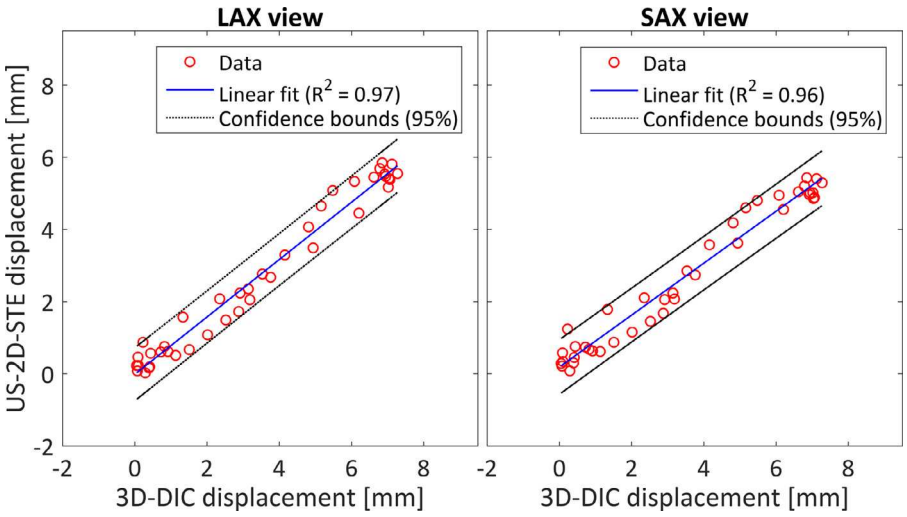

Fig. 4. Displacement data obtained from 3D-DIC versus displacement data obtained from US-2D-STE for the LAX and SAX views. Linear regression plotted with 95% confidence interval.

relative rotation of the coordinate system and uncertainty in ROI location.

Combined US- and DIC-based measurements have already been performed to study the behaviour of biological tissues. Slane et al. [24] used 2D US elastography to quantify motion and strain in *ex vivo* porcine flexor tendons and results strongly correlated with separated surface measurements obtained from 2D-DIC. Moreover, 2D-DIC was used as a reference to validate US strain measurements in *ex vivo* axial loading of human lateral collateral ligaments [23]. Furthermore, Campo et al. [25] compared results from US and 3D-DIC obtained for assessment of the pulse wave velocity in healthy individuals, although they could only compare velocity and acceleration between the two methods as strain was only calculated using 3D-DIC.

Although the adoption of 3D-DIC as a clinical tool poses some challenges such as the development of an effective biocompatible speckle pattern and the requirement for optical access to the heart surface, 3D-DIC has significant potential to provide full-field characterisation of epicardial deformations *ex vivo* at higher temporal and spatial resolution than the current clinical imaging modalities. Moreover, there is a trend to optimise 3D-DIC for real-time dynamic strain measurements [26], which will further enhance its value within the biomedical field.

5. Conclusions

This study presents an experimental framework for multimodal strain imaging in an *in vitro* porcine heart platform that replicates realistic haemodynamic conditions and controlled deformations of the heart. Combined measurements of 3D-DIC and US-2D-STE were carried out to analyse displacement and strain in the heart. 3D-DIC demonstrated high repeatability in assessing the dynamic 3D motion and strain of the LV surface over multiple cardiac cycles unlike US-2D-STE, which is prone to accumulated errors over time that cause a drift in the tracking. Therefore, analysis of displacement and strain was performed over a single cardiac cycle. Results showed a very strong correlation of displacements obtained from the two methods, however, with systematically larger displacement measured by 3D-DIC. Directions of maximum principal strain reconstructed with 3D-DIC showed a distinctive orientation at peak strain, which reflected the distribution of the circumferential and longitudinal strain obtained from US-2D-STE. This study demonstrates the potential of 3D-DIC to perform repeatable and dynamic measurement of displacement and strain during heart deformations providing a localised measurement of strain, which cannot be achieved with US-2D-STE. This supports future applications of this method in *ex vivo* beating heart platforms to give a comprehensive characterisation of epicardial strain resulting from the complex contraction of the heart.

Declaration of Competing Interest

None

Acknowledgements

This work was funded by the European Commission through the H2020 Marie Skłodowska-Curie European VPH–CaSE Training Network (www.vph-case.eu). GA No. 642612.

Ethical approval

All protocols followed by the slaughterhouse and laboratory were consistent with EC regulations 1069/2009 regarding the use of slaughterhouse animal material for diagnosis and research, supervised by the Dutch Government (Dutch Ministry of Agriculture, Nature and Food Quality) and were approved by the associated legal authorities of animal welfare (Food and Consumer Product Safety Authority).

Supplementary materials

Supplementary material associated with this article can be found, in the online version, at doi:10.1016/j.medengphy.2019.09.021.

References

[1] Benjamin EJ, Virani SS, Callaway CW, Chamberlain AM, Chang AR, Cheng S, et al. Heart disease and stroke statistics—2018 update: a report from the American heart association. Circulation 2018;137. doi:10.1161/CIR.0000000000000558.
[2] Tops LF, Delgado V, Marsan NA, Bax JJ. Myocardial strain to detect subtle left ventricular systolic dysfunction. Eur J Heart Fail 2017;19(3):307–13. doi:10.1002/ejhf.694.
[3] Tee M, Noble JA, Bluemke DA. Imaging techniques for cardiac strain and deformation: comparison of echocardiography, cardiac magnetic resonance and cardiac computed tomography. Expert Rev Cardiovasc Ther 2013;11(2):221–31. doi:10.1586/erc.12.182.

[4] Mor-Avi V, Lang RM, Badano LP, Belohlavek M, Cardim NM, Derumeaux G, et al. Current and evolving echocardiographic techniques for the quantitative evaluation of cardiac mechanics: ASE/EAE consensus statement on methodology and indications endorsed by the Japanese society of echocardiography. Eur J Echocardiogr 2011;12(3):167–205. doi:10.1093/ejechocard/jer021.
[5] Sutton MA, Orteu J-J, Schreier H. Image correlation for shape, motion and deformation measurements. Boston, MA: Springer US; 2009.
[6] Palanca M, Tozzi G, Cristofolini L. The use of digital image correlation in the biomechanical area: a review. Int Biomech 2016;3(1):1–21. doi:10.1080/23335432.2015.1117395.
[7] Sutton MA, Ke X, Lessner SM, Goldbach M, Yost M, Zhao F, et al. Strain field measurements on mouse carotid arteries using microscopic three-dimensional digital image correlation. J Biomed Mater Res Part A 2008;84A(1):178–90. doi:10.1002/jbm.a.31268.
[8] Genovese K, Montes A, Martínez A, Evans SL. Full-surface deformation measurement of anisotropic tissues under indentation. Med Eng Phys 2015;37(5):484–93. doi:10.1016/j.medengphy.2015.03.005.
[9] Bersi MR, Bellini C, Di Achille P, Humphrey JD, Genovese K, Avril S. Novel methodology for characterizing regional variations in the material properties of murine aortas. J Biomech Eng 2016;138(7):071005. doi:10.1115/1.4033674.
[10] Soltani A, Lahti J, Järvelä K, Curtze S, Laurikka J, Hokka M, et al. An optical method for the in-vivo characterization of the biomechanical response of the right ventricle. Sci Rep 2018;8(1):6831. doi:10.1038/s41598-018-25223-z.
[11] Ferraiuoli P, Kappler B, van Tuijl S, Stijnen M, de Mol BAJM, Fenner JW, et al. Full-field analysis of epicardial strain in an *in vitro* porcine heart platform. J Mech Behav Biomed Mater 2019;91:294–300. doi:10.1016/j.jmbbm.2018.11.025.
[12] Leopaldi AM, Wrobel K, Speziali G, van Tuijl S, Drasutiene A, Chitwood WR. The dynamic cardiac biosimulator: a method for training physicians in beating-heart mitral valve repair procedures. J Thorac Cardiovasc Surg 2018;155(1):147–55. doi:10.1016/j.jtcvs.2017.09.011.
[13] Leopaldi AM, Vismara R, van Tuijl S, Redaelli A, van de Vosse FN, Fiore GB, et al. A novel passive left heart platform for device testing and research. Med Eng Phys 2015;37(4):361–6. doi:10.1016/j.medengphy.2015.01.013.
[14] Ferraiuoli P, Taylor J, Martin E, Fenner J, Narracott A. The accuracy of 3D optical reconstruction and additive manufacturing processes in reproducing detailed subject-specific anatomy. J Imaging 2017;3(4):45. doi:10.3390/jimaging3040045.
[15] Lecompte D, Smits A, Bossuyt S, Sol H, Vantomme J, Van Hemelrijck D, et al. Quality assessment of speckle patterns for digital image correlation. Opt Lasers Eng 2006;44(11):1132–45. doi:10.1016/j.optlaseng.2005.10.004.
[16] Blaber J, Adair B, Antoniou A. Ncorr: open-Source 2D digital image correlation MATLAB software. Exp Mech 2015;55(6):1105–22. doi:10.1007/s11340-015-0009-1.
[17] Humphrey JD. Cardiovascular solid mechanics. New York, NY: Springer New York; 2002. doi:10.1007/978-0-387-21576-1.
[18] Genovese K, Lee YU, Humphrey JD. Novel optical system for *in vitro* quantification of full surface strain fields in small arteries: I. theory and design. Comput Methods Biomech Biomed Eng 2011;14(3):213–25. doi:10.1080/10255842.2010.545823.
[19] Lopata RGP, Nillesen MM, Hansen HHG, Gerrits IH, Thijssen JM, de Korte CL. Performance evaluation of methods for two-dimensional displacement and strain estimation using ultrasound radio frequency data. Ultrasound Med Biol 2009;35(5):796–812. doi:10.1016/j.ultrasmedbio.2008.11.002.
[20] Lopata RGP, Hansen HHG, Nillesen MM, Thijssen JM, De Korte CL. Comparison of one-dimensional and two-dimensional least-squares strain estimators for phased array displacement data. Ultrason Imaging 2009;31(1):1–16. doi:10.1177/016173460903100105.
[21] Smith BW, Li M, Tong W. Error assessment for strain mapping by digital image correlation. Exp Tech 1998;22(4):19–21. doi:10.1111/j.1747-1567.1998.tb02332.x.
[22] Petterson NJ, Fixsen LS, Rutten MCM, Pijls NHJ, van de Vosse FN, Lopata RGP. Ultrasound functional imaging in an ex vivo beating porcine heart platform. Phys Med Biol 2017;62(23):9112–26. doi:10.1088/1361-6560/aa9515.
[23] Gijsbertse K, Sprengers A, Naghibi Beidokhti H, Nillesen M, de Korte C, Verdonschot N. Strain imaging of the lateral collateral ligament using high frequency and conventional ultrasound imaging: an ex-vivo comparison. J Biomech 2018;73:233–7. doi:10.1016/j.jbiomech.2018.03.035.
[24] Chernak Slane L, Thelen DG. The use of 2D ultrasound elastography for measuring tendon motion and strain. J Biomech 2014;47(3):750–4. doi:10.1016/j.jbiomech.2013.11.023.
[25] Campo A, Soons J, Heuten H, Ennekens G, Goovaerts I, Vrints C, et al. Digital image correlation for full-field time-resolved assessment of arterial stiffness. J Biomed Opt 2014;19(1):016008. doi:10.1117/1.JBO.19.1.016008.
[26] Wu R, Wu H, Arola D, Zhang D. Real-time three-dimensional digital image correlation for biomedical applications. J Biomed Opt 2016;21(10):107003. doi:10.1117/1.JBO.21.10.107003.

Please cite this article as: P. Ferraiuoli, L.S. Fixsen and B. Kappler et al., Measurement of in vitro cardiac deformation by means of 3D digital image correlation and ultrasound 2D speckle-tracking echocardiography, Medical Engineering and Physics, https://doi.org/10.1016/j.medengphy.2019.09.021